

ABOUT INITIAL SOLIDIFICATION IN CONTINUOUS CASTING OF STEEL

W. Kurz

High solidification velocities, high temperature gradients and strong melt flow characterize the first moments of solidification in a continuous caster. The beginning of shell growth in the meniscus area is determined by the local heat flow, the strength of the shell and the fluid dynamics. In this region of the process, surface defects such as oscillation marks form, which influence the shell growth processes in the mould. Phase (ferrite/austenite) and microstructure selections (cells/dendrites) operate in this part of the process and control microsegregation, mechanics and defects of the surface region of the product. One of the most serious problems is hot cracking and a proper control of the casting parameters and of the steel composition is essential for obtaining high quality products. Stainless steels are highly sensitive to these phenomena. Control of deformation of the solid with a mushy zone is also of great importance as it is an input for machine design.

KEYWORDS: oscillation marks, meniscus, rapid solidification, phase selection, shell strength, hot cracking

INTRODUCTION

The quality of continuous casting steel depends very much on the control of the solidification conditions in the copper mould. There the hot melt enters in contact with the water-cooled mould and starts solidifying. Convective flow, slag-metal interaction, meniscus shape, heat extraction, surface waves, oscillation of the mould, etc. influence the first millimeters of the solid shell and leave their imprint on the surface of the casting.

Already more than 50 years ago, Thornton [1] published experimental observations of solidification and deformation of the meniscus during ingot casting of low melting point metals and steel. Reviews of the work of others during the early years can be found in [2] and [3]. In-between substantial progress has been made in the understanding of the various phenomena which are responsible for the formation of defects such as surface marks or hot cracks (see Lesoult et al. [3]).

The objective of this paper is to present some key elements of understanding the process fundamentals of the last 3 decades as far as they relate to the formation of the skin and its defects. It is neither intended

to give a detailed historic view nor a general and coherent theory of the phenomena. Instead, it will be shown which methods led and are still leading to a better knowledge of the system for an improved product quality. Numerical methods which play an essential part in this endeavor are subject of other reviews.

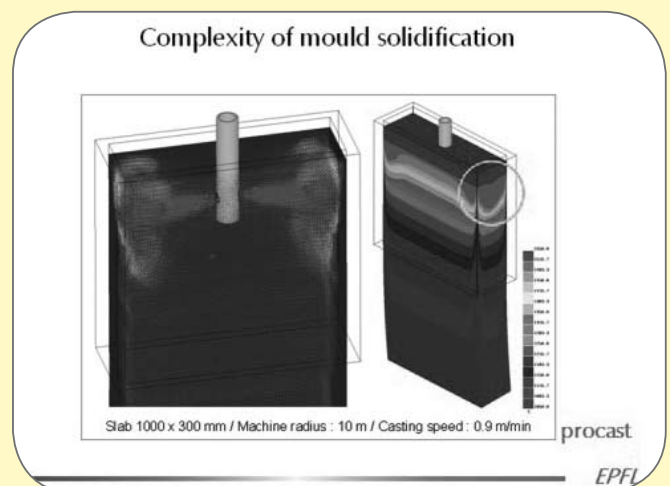
This paper starts with a review of certain aspects of research which has been undertaken at EPFL in collaboration with Concast some 30 years ago. Later work at EPFL on microstructure and phase selection as well as on hot cracking will also be discussed in view of presenting a sufficiently complete methodology for the optimization of product quality in continuous casting. More recently, this topic has found renewed interest, promising another era of progress. Important results of this research are also included in the present text.

INITIAL STAGES OF SOLIDIFICATION

Solidification in the mould

The results of coupled numerical mod-

elling of fluid flow and heat flow (Fig. 1), show nicely that convection in the melt and contact of the liquid with the copper mould produce a complex temperature field [4]. In this region, large thermo-mechanical constraints are built up and lead to deformation and often also to cracking. Further, due to the huge temperature difference between the melt and the water-cooled mould of some 1400 K, wetting of the liquid is not possible and a convex meniscus forms. The solidification behaviour of this meniscus region is fun-



▲
Fig. 1

Flow and temperature field calculation of liquid steel solidifying in a water cooled copper mould (Ludwig et al., Calcom-ESI [4]).

Wilfried Kurz

EPFL, the Swiss Federal Institute
of Technology Lausanne
1015 Lausanne, Switzerland

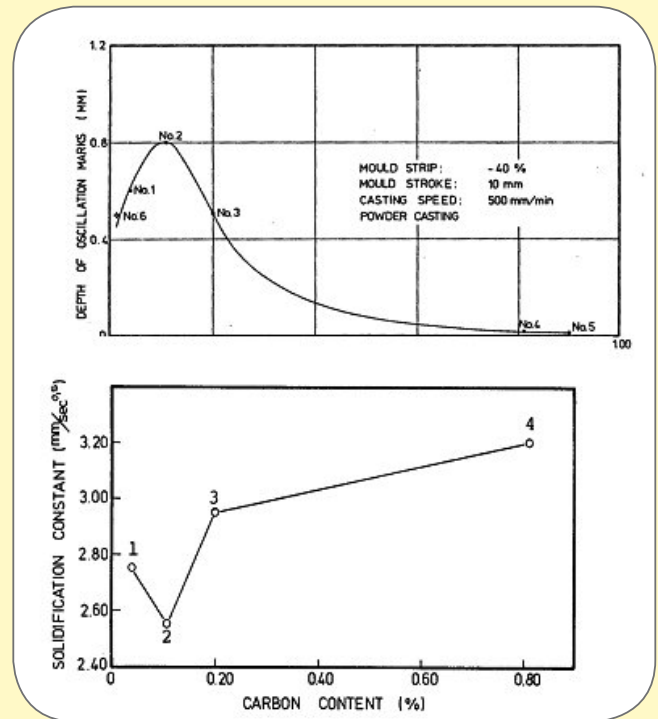
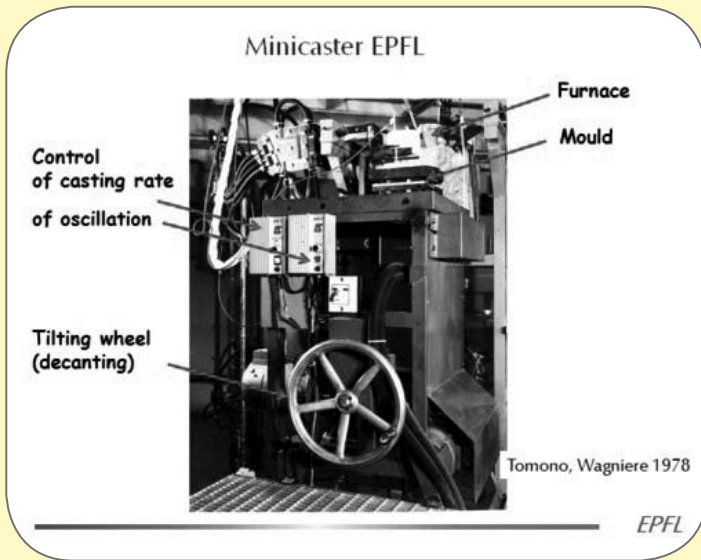


Fig. 2 Minicaster for the simulation of the first stages of solidification in the continuous casting process. The mould could be tilted for decanting the liquid [5].

Fig. 5 Depth of oscillation marks (upper diagram) and solidification constant for parabolic growth as a function of the carbon content [5].

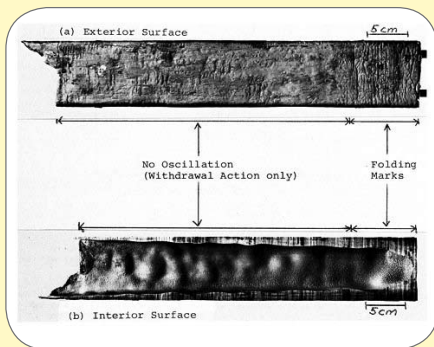


Fig. 3 External and internal surfaces of a 0,17 % C-steel billet cast without mould oscillation [5,6].

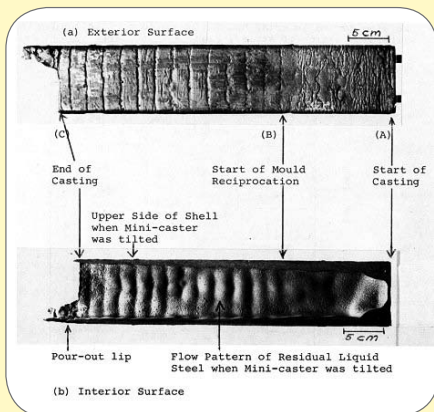


Fig. 4 External and internal surfaces of a 0,17 % C-steel billet cast with mould oscillation [5,6].

damental for the surface quality and in consequence for the solidification conditions. The sequence of events of the initial solidification which are interrelated is the following:

Meniscus solidification ↔ surface formation ↔ local gap formation ↔ heat flow ↔ local solidification conditions ↔ microstructure of skin ↔ phase selection ↔ microsegregation ↔ shell deformation ↔ hot cracking. In order to study mechanisms of surface formation a "minicaster" has been built in the late 70s, Fig. 2 [5]. The minicaster consisted of a 700 mm long 85 mm square billet mould. During the casting operation, the mould was filled and then tilted for decanting the liquid metal. In this way, the outer and corresponding inner surface could be observed. Castings were produced with and without mould oscillation and using different steels with carbon contents between 0,01 and 0,91 wt%. Commercial casting powder was used as lubricant. Without mould oscillation, the external surface of the billet in a 0,17 % C-steel and its counterpart, the decanted solid-liquid interface, were very irregular and showed finely spaced marks, which were called folding marks, Fig. 3. With mould oscillation, the same steel showed narrow spaced folding marks together with deeper oscillation marks, Fig. 4. A good correspondence of the depressions in the solid liquid

interface (lower photo of Fig. 4) with the marks at the outer surface (upper photo) can be observed [6]. The upper diagram of Fig. 5 shows the depth of the oscillation marks as a function of the carbon content. The difference in the contact area between steel and copper leads to a corresponding variation of the solidi-

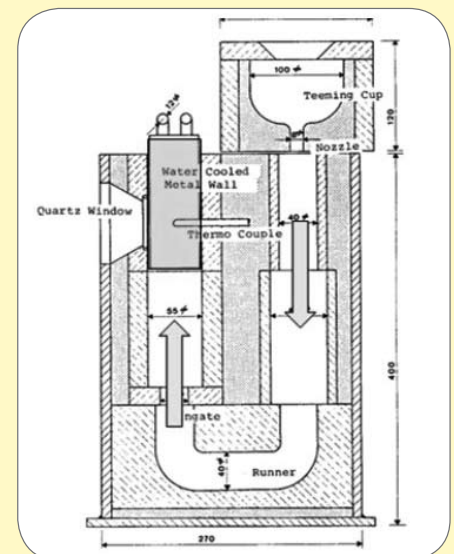
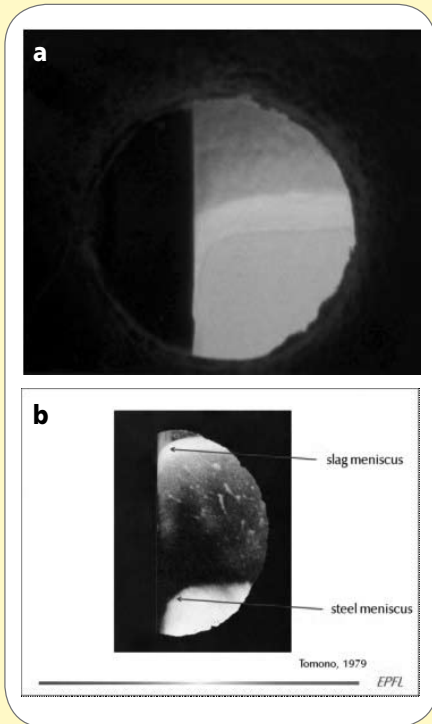


Fig. 6 Chill casting mould with window for meniscus observation [8].



▲
Fig. 7
Menisci during bottom pouring: (a) liquid steel in contact with chill, (b) liquid slag and steel in contact with chill [6,8].

fication constant for parabolic growth ($K=d/\sqrt{t}$, with d the shell thickness in mm and t the solidification time in s). The growth rate of the solid was high when the marks were shallow and low when the marks were well developed [5]. Such experiments have been made also with succinonitril, an organic model substance, which allows direct observation of the phenomena [5-7]. Mazet and Lesoult varied the mould temperature in a wide range and showed the effect of the



▲
Fig. 9
Hook inside a folding mark [8].

liquid-mould contact angle on surface quality [7].

Folding Mark Formation

In order to study the mark mechanism without oscillation of the mould in more detail, a bottom pouring device with a copper chill was built, allowing the observation of the meniscus dynamics through a quartz window, Fig. 6. Fig. 7a gives an oblique view on the steel meniscus through the window, with the lower trace in contact with the window in the front and the upper trace at the rear wall of the mould. When the casting was performed with a slag layer on top of the steel, two menisci could be seen (Fig. 7b). Filming the experiments allowed observa-

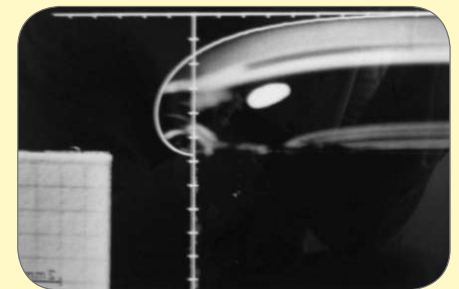
tion of mark formation by overflow. Fig. 8 is a schematic representation of such an overflow mechanism. In Fig. 9, the trace of the solidified meniscus inside the casting can be seen. In recent work, this trace is called "hook" [3,9].

Recently Sengupta et al. [9] have also undertaken such experiments and found that (i) hooks form by dendritic solidification of the meniscus during the negative strip time, and (ii) oscillation marks form by flow of the melt over the hook and consecutive solidification of the liquid.

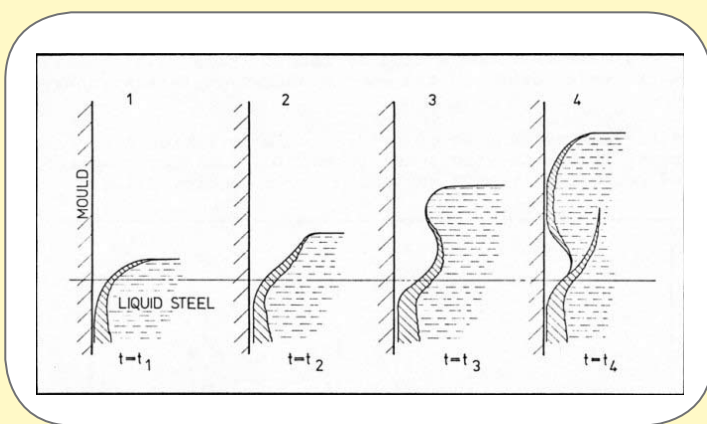
In 1982 Stemple et al. [2] published results on the effect of surface waves on folding marks (which they called ripples) in Sn-Pb alloys. These authors applied a static magnetic field to the casting and showed that ripple formation was strongly reduced.

Meniscus shape

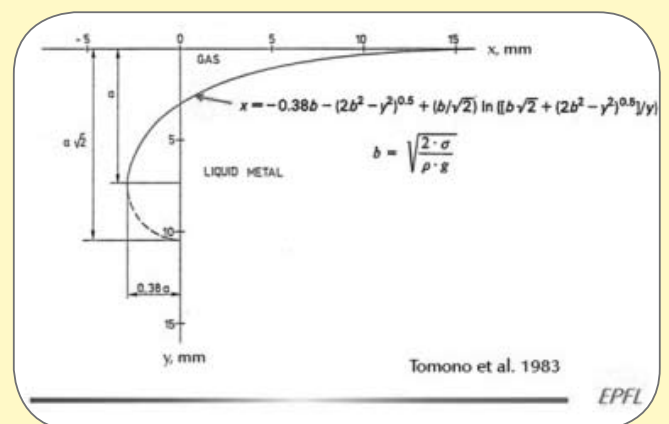
As the meniscus is the controlling part of the problem, it was necessary to understand its form. The photo of a water meniscus just before the moment of overflow from a non-wetting container (Fig. 10) shows very clearly the form which is repre-



▲
Fig. 10
Water meniscus forming during overflow in a non-wetting container [10].



▲
Fig. 8
Folding mark formation by overflow [6].



▲
Fig. 11
Theoretical form of a liquid cylinder on a non-wetting horizontal surface [8, 11].

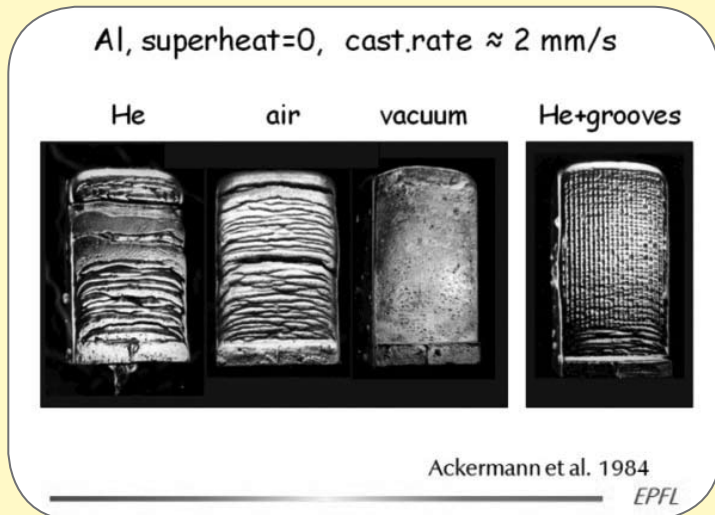


Fig. 14

Mark formation map showing the effect of casting rate, melt superheat and heat flux on the limit above which no mark formation occurs [12].

Helium increases the heat flux and deteriorates the surface, while vacuum (10^{-4} Torr) decreases the cooling effect and leads to a smooth surface. Vertical grooves machined into the copper mould with a spacing which, due to surface tension, did not allow the melt to penetrate, led also to a substantial reduction of the heat flow and produced, even in the presence of helium, a folding-mark free casting. Heat flow calculations were confronted

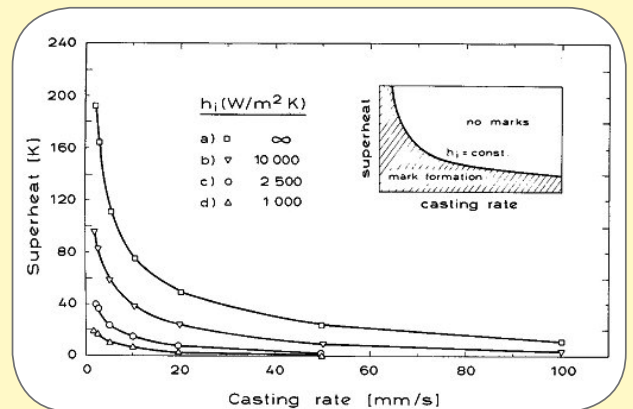


Fig. 12

Chill castings under different atmospheres and chill morphologies [12].

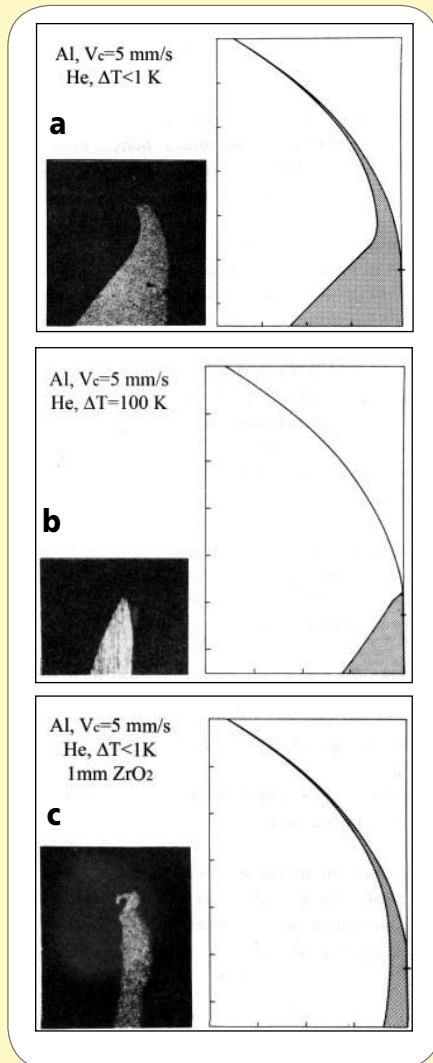


Fig. 15

Local solidification conditions for steel in the Cu-mould (numerical results [16]).

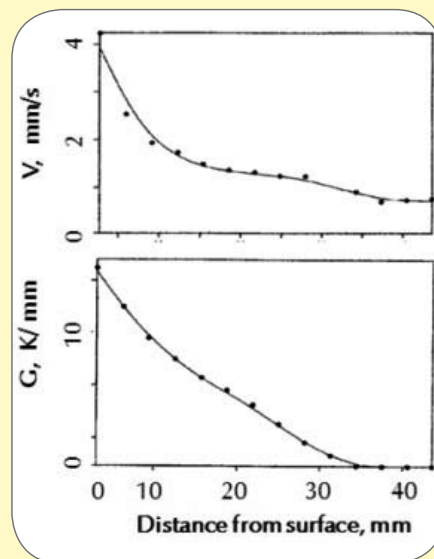


Fig. 13

Decanted and calculated initial solid in Al chill castings under He atmosphere. ΔT values indicate the superheat of the melt [12,13]. Note that the very first solid film along the meniscus is very weak, deforms easily and is carried away in the decanting operation.

sented by the equation in Fig. 11. If a vertical wall comes in contact with this meniscus only the upper part of the curve is real. For a better understanding of the param-

eters which influence the folding marks, tin and aluminum castings have been performed in a vacuum furnace which allowed the control of the atmosphere in the me-

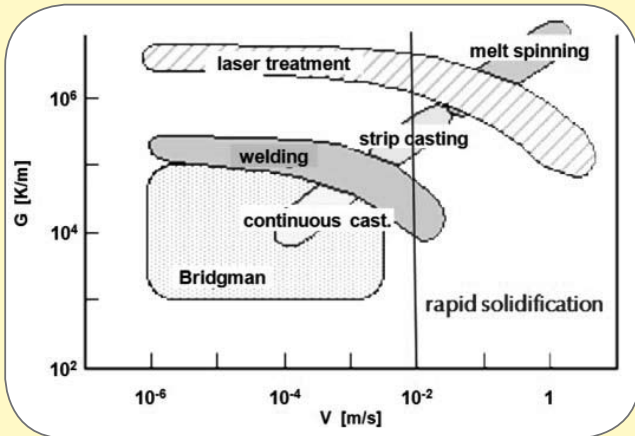
with decanted shells (Fig. 13 [13]). If the meniscus solidified as in (a), mark formation was observed, while in the case of a highly superheated melt (b) no meniscus solidification took place, this producing a smooth surface. Case (c) with a ceramic coating, is intermediate and shows only weak marks.

The casting rate has also an influence on mark formation. In Fig. 14 its effect, together with the superheat of the melt and heat flow in the mould can be seen. Clearly, a high superheat of the melt is not a solution in practice as it will promote extended columnar growth.

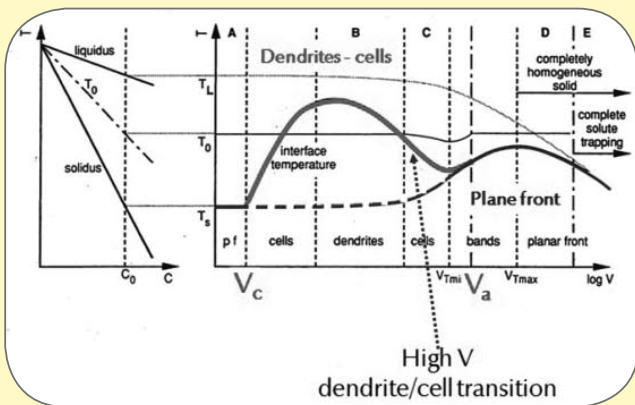
Dip tests have also been developed in order to simulate the initial solidification behaviour in the mould [14,15]. This type of experiment is much easier to undertake than the more realistic experiments in a mould. Due to the contraction of the specimen onto the dip-mould, the steel experiences, however, a different heat flow which results in different microstructures and mechanical behaviour.

LOCAL SOLIDIFICATION CONDITIONS

The contact between the casting and the copper mould determines the heat flux and the latter the local solidification conditions. Fig. 15 indicates the variation of the solidification front velocity, V , and the interface temperature gradient, G [16]. According to these calculations, the veloc-



▲ Fig. 16 Processing map showing the range of G- and V-values for various solidification processes.



▲ Fig. 17 Interface response (growth temperature as a function of V) for an alloy composition C_0 [18,20].

ity at the surface is of the order of 4 mm/s while the temperature gradient is around 15 K/mm, leading to a cooling rate of some 60 K/s. Fig. 16 gives an overview of different solidification processes with positive temperature gradients in a V-G diagram. Conventional continuous casting processes are below the limit of rapid solidification while the high velocity casting processes such as strip casting, melt spinning and the laser treatment processes are above this limit, the latter being defined by the loss of local equilibrium. Rapid solidification theory is therefore of interest for many casting processes but only at the very beginning of conventional continuous casting.

RAPID SOLIDIFICATION

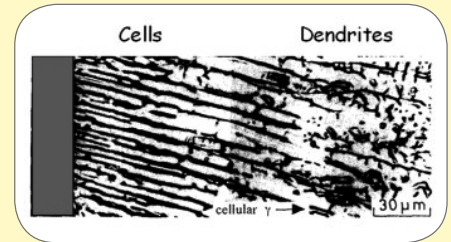
Generally, solidification conditions in alloys lead to dendritic or cellular microstructures. The atomic processes at the solid-liquid interface are rapid enough to allow local equilibrium to establish, i.e. at

the very interface the phase diagram can be applied [17-19]. With increasing interface velocity, the microstructure becomes refined, dendrites change to cells and, at very high rates, local equilibrium is progressively lost and plane front growth is observed. Fig. 17 sketches the microstructure evolution for a given alloy and G-value in steady state with the aid of the interface temperature [20]: At low velocities (below the limit of constitutional undercooling, V_c) and at high velocities (above the limit of absolute stability, V_a) the solid-liquid interface assumes plane front morphology (indicated by the uninterrupted curve) and grows at solidus. Inbetween both limits dendritic and cellular structures prevail. In Fig. 18, the cell to dendrite transition with increasing distance from the chill (decreasing velocity) can be observed [21].

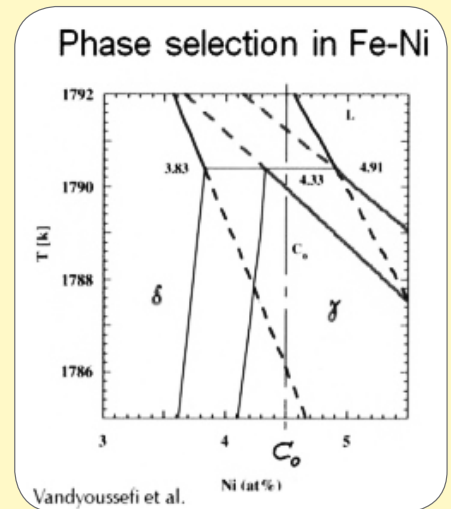
The curves in Fig. 17 represent the Interface Response (IR) to a varying interface velocity. The IR allows the determination of the observed phases if there is more than one to compete with each other, for example alpha or gamma in austenitic steels (see below). Each phase has its IR and, if nucleation is abundant, the phase with the highest tip temperature will form preferentially. The chill technique employed by Mizukami et al. [21] allows the observation of the very first contact of the melt with the mould. Such experiments are helpful for the interpretation of microstructures obtained in strip casting processes [22].

PHASE SELECTION

Work on solidification microstructure and phase selection maps has produced a simple and generally useful model for the optimization of alloy composition (including effects of trace elements) and processing conditions in view of achieving the right microstructure [20,23]. Following this ap-



▲ Fig. 18 High-V cell to dendrite transition at 110 μm from the Cu-chill (see fig. 17) [21].



▲ Fig. 19 Peritectic Fe-Ni phase diagram with stable (continuous lines) and metastable equilibria (interrupted lines).

proach and using the models of Fig. 17, it is possible to control the phase formation such as delta or gamma iron in Fe-Ni alloys or in commercial 18-8 stainless steels. For example, Fig. 19 shows the Fe-Ni peritectic with its stable and metastable equilibria. With the aid of the theory sketched in Fig. 17 and the phase diagram information of Fig. 19, the growth rate range in which delta or gamma iron forms can be calculated. Both phases have a specific IR. The phase which is selected is characterized by the highest dendrite tip temperature. According to Fig. 20, ferrite will be observed at low velocities, while at high growth rates austenite will form [27]. These results can be combined in a phase selection map (Fig. 21) which shows that the ferrite austenite transition is a function of the Ni-composition. For a linear phase diagram, the transition velocity can be calculated by the equation given in Fig. 22. For details of this calculation, the reader is referred to a paper by Umeda et al. [23].

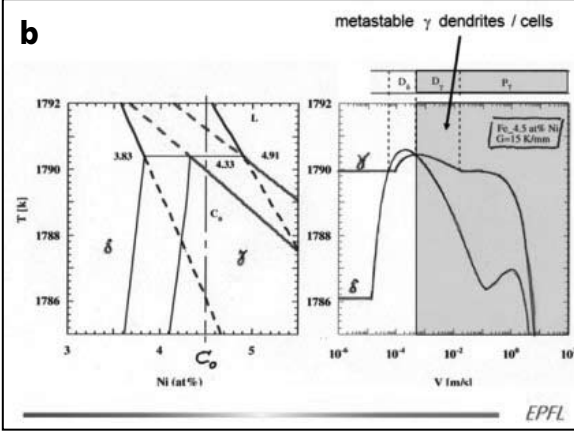
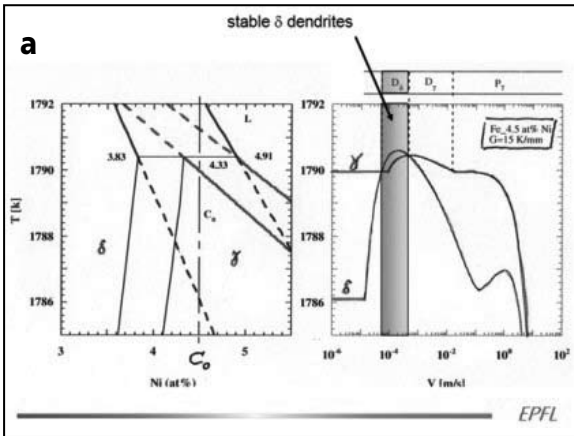


Fig. 20 Interface response for delta ferrite and gamma austenite. (a) at low velocity delta grows at the higher temperature and is formed while (b) at high velocities gamma has a kinetic advantage over delta iron [27].

Peritectic Phase Selection

$$V_{tr}^{\alpha/\beta} \cong \sigma^* D \left(\frac{\Delta T_m^{\alpha/\beta} + C_0 \Delta m^{\alpha/\beta}}{(\Delta T_0^{\alpha} k^{\alpha} \Gamma^{\alpha})^{1/2} - (\Delta T_0^{\beta} k^{\beta} \Gamma^{\beta})^{1/2}} \right)^2$$

EPFL

Fig. 22 Transition velocity as a function of composition for linearized phase diagrams [23].

δ - γ transition in Fe-18Cr-8Ni

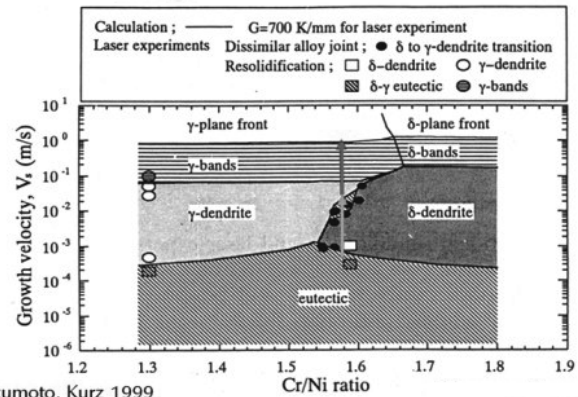


Fig. 23 Phase and microstructure selection map for ternary Fe-Cr-Ni alloys. The ferrite-austenite transition curve has been verified by laser experiments [24-26].

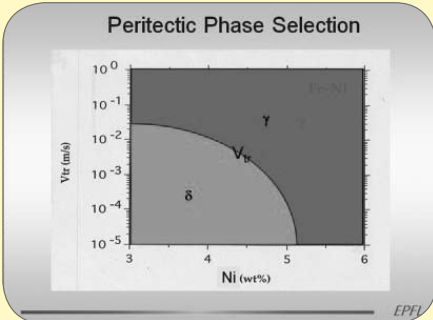
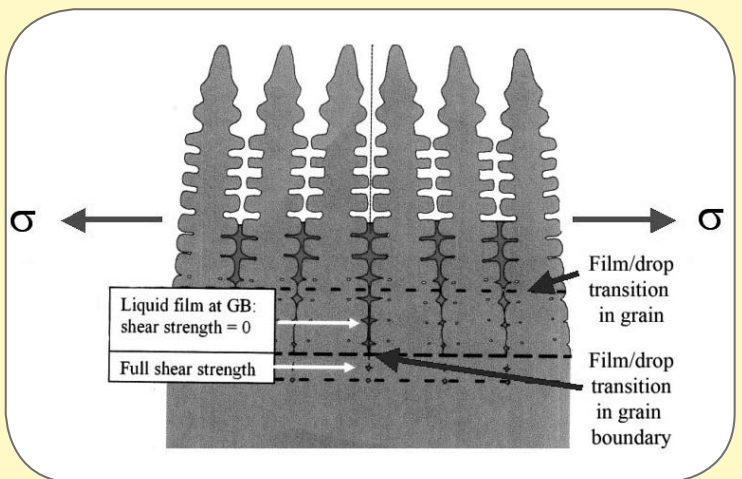


Fig. 21 Phase selection map for binary Fe-Ni alloys.

Fig. 24

Microstructure of the shell with two dendritic grains and one grain boundary in the centre [31].



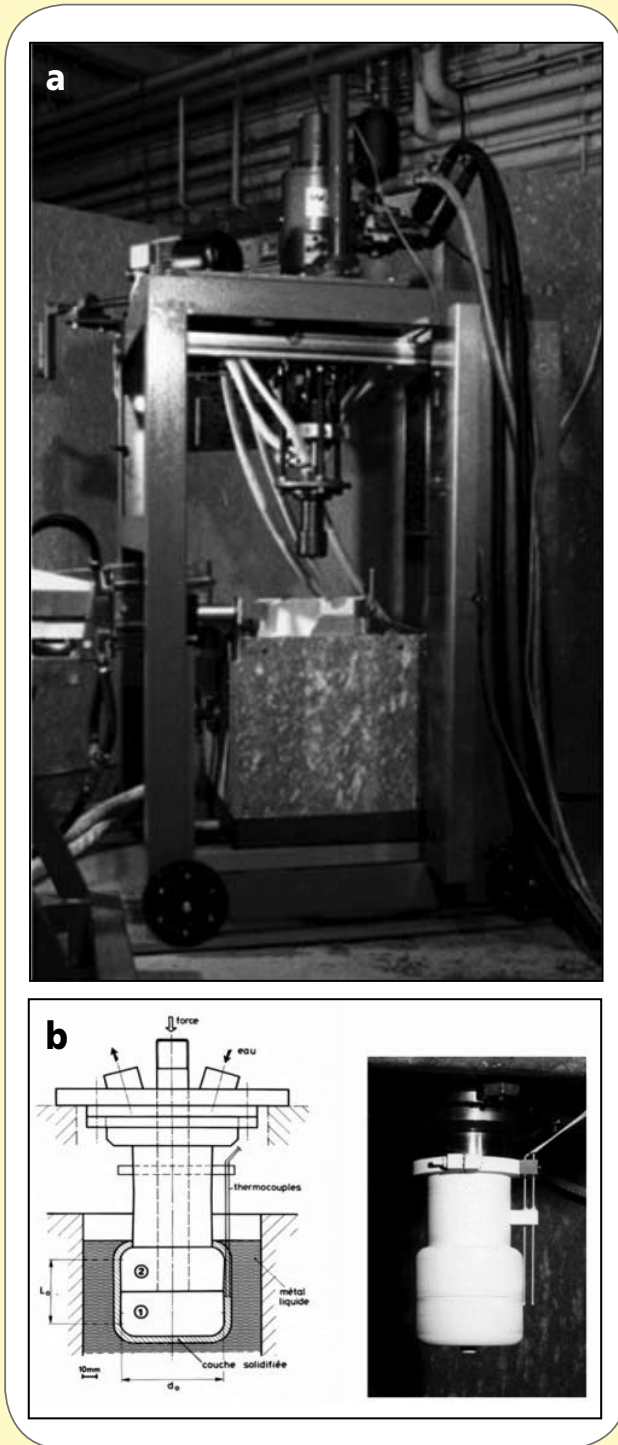
Ternary alloys are a step in the direction of technical alloys. Fig. 23 shows calculations and experimental points for Fe-Cr-Ni alloys [24-26] which form the basis of austenitic stainless steels. Cases that are practically more interesting are technical alloys, such as stainless steels. Using thermodynamic databases, real steels with half a dozen elements have been

modelled and successfully compared to experimental findings [28].

MECHANICAL BEHAVIOUR OF THE SHELL

Surface defects which are characterized by marks, inclusions and cracks depend essentially on the mechanical behaviour

of the first shell to form. As the solid is composed of a mushy zone and a fully solid plate (Fig. 24), its mechanics is complex [29]. In tension, transverse to the dendrite axis, the mushy zone has essentially no strength. The reason for this behaviour lies in the presence of interdendritic and intergranular liquid films, which have zero shear strength. The shell



▲
Fig. 25
In situ tensile test equipment; (a) apparatus, (b) split chill with ceramic coating, [32].

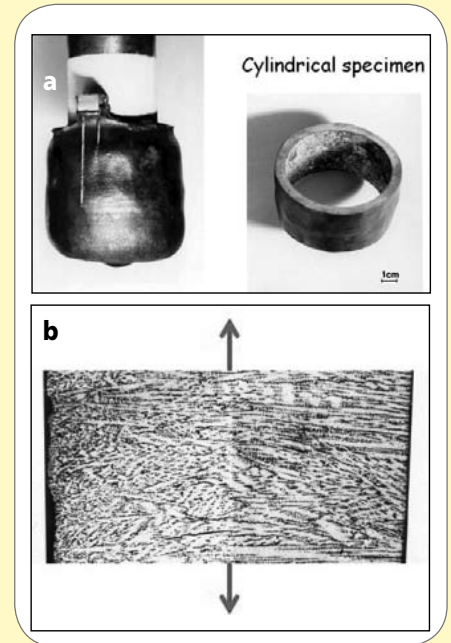
is composed of four regions, each showing a different morphology and mechanical behaviour; (i) region of easy feeding (white interdendritic liquid in Fig. 24), (ii) region of restricted interdendritic flow due to densification of dendritic network and liquid film formation (dark grey in Fig. 24), (iii) region of liquid drops in the

grains (in blue) and films in the grain boundaries, (iv) region of liquid drops in grains and boundaries, and (v) fully solid region. Only beyond the morphological transition from films to drops in the grain boundaries which happens close to $f_s = 1$, the solid recovers its full strength. There is therefore a sharp transition of properties around this critical volume fraction solid.

Note that the corresponding temperature is below the equilibrium solidus and its value depends on microsegregation, solid state diffusion, dendrite morphology and grain boundary energy [30].

To measure the mechanical strength of the solidifying shell an "in-situ" tensile test was developed in the early 1980s (Fig. 25a [32]). A cylindrical split copper chill (Fig. 25b) was lowered into the liquid metal. After a given time to allow growth of the shell, typically 10 to 20 s, the copper cylinder was separated and a force vs. time (displacement) diagram was recorded [32,33]. For more regular shell solidification and less friction, the Cu was coated with a thin ceramic layer (Fig. 25c). After pullout from the melt, the solidified steel shell was machined and separated from the

chill. Fig. 26 shows the shell with thermocouples for temperature measurements (Fig. 26a) and the microstructure of the shell (Fig. 26b). Typical tensile test results are shown in Fig. 27. In Fig. 27a, a force-time diagram [34] is presented. The coordinates can be easily converted into stress-strain curves, which, for other experiments, are shown in Fig. 27b [35, 36]. Over the years, this test has been developed further and used to characterize many steel grades by the group of C. Bernhard from the University of Leoben. These authors called it "submerged split

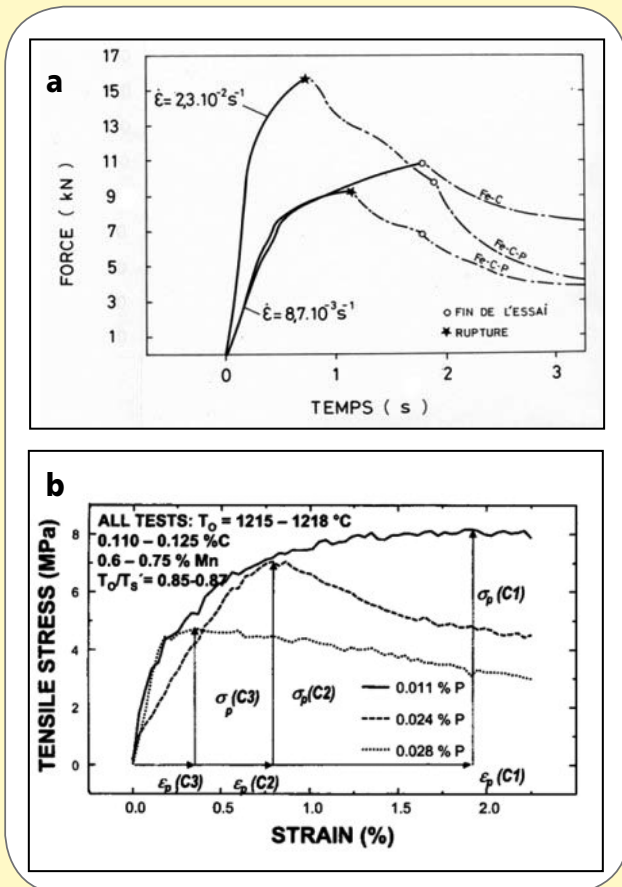


▲
Fig. 26
In-situ tensile test specimen; (a) after pull out from the melt (left) and after machining (right); (b) columnar dendritic microstructure transverse to the stress axis [33,34].

chill tensile" (SSCT) test [35-39]. In the same period, B.G. Thomas and his group developed a numerical elasto-viscoplastic thermal stress model. They took into account shrinkage and solid-state transformations [29]; in this paper, they give also an overview of relevant work in this area. Further work on shrinkage and stress in the SSCT test has been performed by Bernhard and Xie [40].

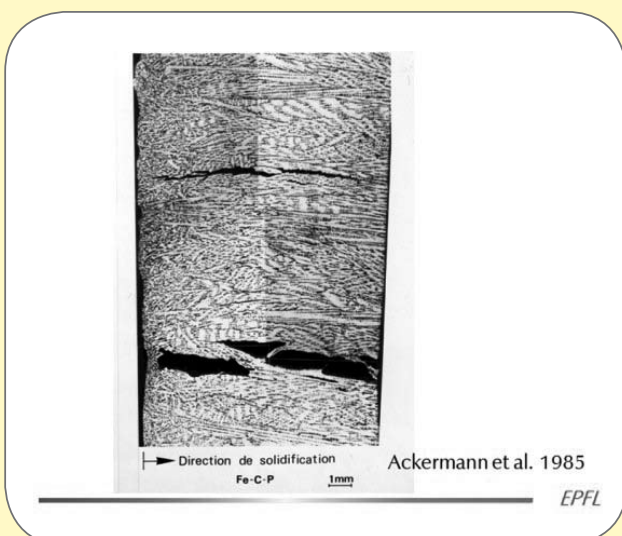
HOT CRACKING

Hot (or solidification) cracking is a phenomenon where shear deformation of the nearly fully solid metal, containing connected liquid films, forms an elongated pore by cavitation, which develops into a crack. Only a narrow temperature interval is responsible for crack opening, i.e. the zone where liquid feeding is too slow to compensate for the deformation but where shear deformation is still possible (volume fraction range of the order of 0.9 to 0.95). It depends largely on alloy composition and phase diagram. Fig. 24 shows details of the mushy zone with the grain boundary forming the vulnerable part of the material as, due to the grain boundary energy, it extends over a larger temperature interval than the intragranular liquid films [30]. Deformation is therefore localized at the grain



▲ Fig. 27

Tensile test curves of solidifying steel; (a) Fe-0.6%C, Fe-0.6%C-0.012%P, Ackermann et al. 1985 [34]; (b) 0.11%C steel with increasing P-content as indicated, Bernhard et al. 2000 [36].



▲ Fig. 28

Hot cracks in steel strained during solidification, Fe-0.6%C-0.012%P [34].

boundaries, which open up at first. Fig. 28 shows a good example of such cracking, which has been produced by a small addition of P to the steel [34].

Bernhard et al. undertook much valuable work to characterize the hot cracking tendency of carbon steels [36,38,39]. Fig. 29 shows results of research in which four different hot cracking models have been confronted with results from the SSCT test. The authors found that these models represent the experimental results quite well up to 0.3 %C but show a qualitatively different behaviour at higher carbon levels. They propose to use a critical strain criterion for judging the hot cracking sensitivity.

CONCLUSION

Much work on experimental and theoretical modelling of the various elements of the early stages of the continuous casting process has been undertaken over the last 30 years. This has led to a better understanding of the basic phenomena which, in this critical region of the process, are instrumental for an optimal product quality.

Four main topics have been treated in this review: Surface mark formation, phase selection during solidification, mechanical behaviour of the shell and hot cracking.

- Formation mechanisms of surface marks: folding and oscillation marks have been produced and observed through a window and deformation and overflow mechanisms studied. The importance of the meniscus shape and heat flow has been

shown. A proposal for a better heat flow control in the meniscus region has been given, e.g. by a grooved mould.

- Phase selection: The selection of ferrite vs. austenite has been treated with

microstructure selection theory. Measures to choose the optimal alloy composition and solidification conditions for reducing the initial austenite fraction have been indicated.

- Mechanical behaviour: Strength and deformation behaviour of the mushy zone with its complex morphology is fundamental for machine design. Some 25 years ago, an apparatus has been developed which allows in-situ measurements of these properties. Recent work with this equipment has produced a number of valuable results for better machine design.

- Hot cracking: Hot cracking depends strongly on the presence of austenite during the first moments of solidification. This phase produces increased segregation of trace elements such as P which substantially increases the crack-sensitive temperature interval. Reduction of hot cracks through a control of the austenite fraction by composition control has become possible and, under others, is very useful for high quality strip casting of stainless steels.

Research in these fields is still ongoing and promises new results for better steels in the future.

ACKNOWLEDGEMENT

The author acknowledges the precious collaboration of Jean-Daniel Wagniere in the experiments.

REFERENCES

[1] D.R. Thornton: "An Investigation on the Function of Ingot Mould Dressings", J. Iron Steel Inst. 183 (1956) 300-315
 [2] D.K. Stemple, E.N. Zulueta, M.C. Flemings: "Effect of Wave Motion on Chill Cast Surfaces", Metall. Trans. 13 B (1982) 503-509
 [3] G. Lesoult, J.-M. Jolivet, L. Ladeuille, Ch.-A. Gandin: Contributions to the Understanding of the Formation of the Skin During Continuous Casting of Steel", in Solidification Processes and Microstructures - A Symposium in Honor of Wilfried Kurz, M. Rappaz, Christoph Beckerman, R. Trivedi eds, TMS 2004, p. 15-26
 [4] O. Ludwig, M. Aloe, P. Thevoz: "State of the Art in Modelling of Continuous Casting", CD-rom Proceedings of the 6th European Conference on Continuous Casting, AIM (2008)
 [5] H. Tomono: "Elements of Oscillation Mark Formation and their Effect on Transverse Fine Cracks in Continuous Casting of Steel", PhD Thesis, EPFL 1979
 [6] H. Tomono, P. Ackermann, W. Kurz, W.

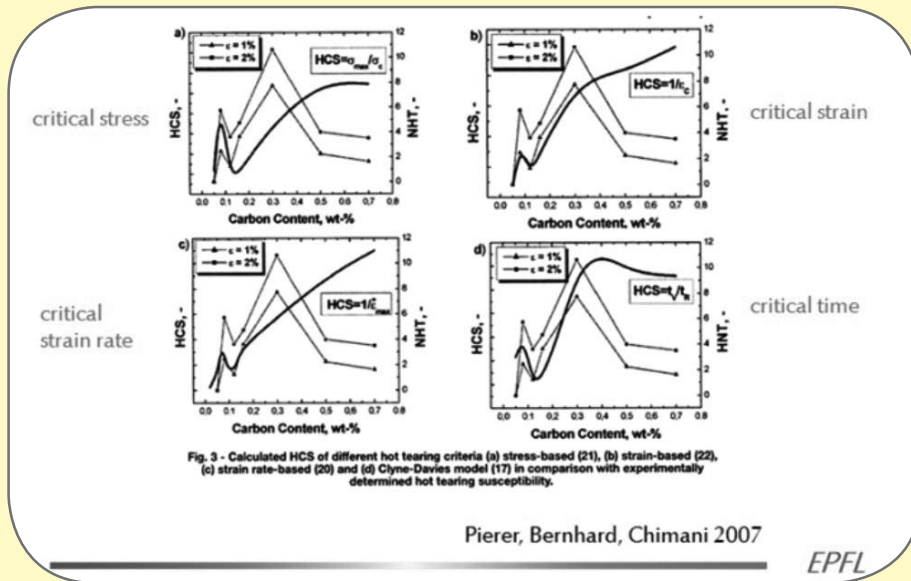


Fig. 29

Comparison of calculated hot cracking sensitivity (dark curve) with SSCT results (dots connected by thin lines). Four different models have been used for the calculations [39].

Heinemann: "Elements of surface mark formation in continuous casting of steel", Proc. Int. Conf. on "Solidification Technology in the Foundry and Casthouse", Univ. Warwick, the Metals Society 1983, 524-531

[7] F. Mazet, G. Lesoult: Rev. Metall.-CIT/Sci. Gen. Matériaux (1994) 1296

[8] H. Tomono, W. Kurz, W. Heinemann: "The liquid steel meniscus in moulds and its relevance to the surface quality of castings" Met. Trans. 12 B (1981) 409-411

[9] J. Sengupta, B.G. Thomas, Ho-Jung Shin, Go-Gi Lee, Seon-Hyo Kim: A New Mechanism of Hook formation during Continuous Casting of Ultra-Low-Carbon Steel Slabs", Metall. Mater. Trans. 37 (2006) 1597-1611

[10] H. Tomono, Kurz 1978 unpublished

[11] J.J. Bikerman: Physical Surfaces, Academic Press, London, 1970

[12] P. Ackermann, W. Heinemann, W. Kurz: "Surface quality and meniscus solidification in pure chill cast metals", Arch. Eisenhüttenw. 55 (1984) 1/8

[13] P. Ackermann, « Processus de formation de marques de surface, typique de la coulée en lingotière fortement refroidie », PhD Thesis, EPFL 1983

[14] Badri, A.; Natarajan, T.T.; Snyder, C.C.; Powers, K.D.; Mannion, F.J.; Cramb, A.W.: "A Mold Simulator for the Continuous Casting of Steel: Part I. The Development of a Simulator", Metall. Mater. Trans. 36B (2005) 355

[15] Badri, A.; Natarajan, T.T.; Snyder, C.C.; Powers, K.D.; Mannion, F.J.; Byrne, M.; Cramb, A.W.: "A Mold Simulator for

Continuous Casting of Steel: Part II. The Formation of Oscillation Marks during the Continuous Casting of Low Carbon Steel", Metall. Mater. Trans. 36B (2005) 373-383

[16] N.M. Vanaparthi, Malur N. Srinivasan: "Modelling of Solidification Structure of Continuous Cast Steel", Modelling Simul. Mater. Sci. Eng. 6 (1998) 237-249

[17] W.J. Boettinger, S.R. Coriell, R.F. Sekerka: Mater. Sci. Eng., 65 (1984) 27

[18] R. Trivedi, W. Kurz: "Dendritic growth", Int. Mater. Rev., 39 (1994) 49/74

[19] W. Kurz, D.J. Fisher: Fundamentals of Solidification, Tech Trans, Switzerland, 4th ed. 1998

[20] W. Kurz "Solidification microstructure - processing maps: Theory and application" Adv. Eng. Materials, 3 (2001) 443-452

[21] H. Mizukami, T. Suzuki, T. Umeda, W. Kurz: Mater. Sci. Eng. A173 (1993) 363-366

[22] T. Emi, H. Fredriksson: "High Speed Continuous Casting of Peritectic Carbon Steels", Mater. Sci. Eng. A413-414 (2005) 2-9

[23] T. Umeda, T. Okane, W. Kurz: "Phase Selection during Solidification of Peritectic Alloys", Acta Mater. 44 (1996) 4209-16

[24] S. Fukumoto, W. Kurz: "On the Alpha to Gamma Transition in Fe-Cr-Ni Alloys during Laser Treatment", ISIJ-International 37 (1997)677-684

[25] S. Fukumoto, W. Kurz: "Prediction of the Alpha to Gamma Transition in Austenitic Stainless Steels during Laser Treatment", ISIJ International 38 (1998) 71-77

[26] S. Fukumoto, W. Kurz: "Solidification phase and microstructure selection maps for Fe-Cr-Ni alloys", ISIJ International 39 (1999) 1270-79

[27] M. Vandyoussefi, H.W. Kerr, W. Kurz: "Solidification microstructure selection map for Fe-Ni peritectic alloys", in Solidification Processing 1997, J. Beech, H. Jones, eds., Dep. Eng. Mater., Univ. Sheffield, Sheffield, 1997, p. 564-567

[28] EPFL, unpublished work

[29] Ya Meng, Chunsheng Li, Jon Parkman, B.G. Thomas: "Simulation of shrinkage and stress in solidifying steel shells of different grades", in Solidification Processes and Microstructure- A Symposium in Honor of Wilfried Kurz, M. Rappaz, Christoph Beckerman, R. Trivedi eds, TMS 2004, p. 33-39

[30] M. Rappaz, A. Jacot, W. J. Boettinger: "Last-stage solidification of alloys: Theoretical model of dendrite-arm and grain coalescence", Metallurgical and Materials Transactions 34 (2003) 467-479

[31] N. Wang, S. Mokadem, M. Rappaz, and W. Kurz: "Solidification cracking of superalloy single- and bi-crystals", Acta Materialia, 52 (2004) 3173-3182

[32] J.-D. Wagniere, P. Ackermann: „Le laboratoire d'aujourd'hui pour les brames de demain", Revue Polytechnique (Switzerland) No 1464, 6(1985) 669-673

[33] P. Ackermann, W. Kurz, W. Heinemann: "In-situ testing of solidifying aluminium and Al-Mg shells", Mater. Sci. Eng. 75 (1985) 79-86

[34] P. Ackermann, J.-D. Wagniere, W. Kurz, EPFL1985, unpublished work

[35] C. Bernhard, H. Hiebler, M.M. Wolf: „Simulation of Shell Strength Properties by the SSCT Test", ISIJ Intern. 36 (1996) suppl., pp S163-S166

[36] C. Bernhard, H. H. Hiebler, M.M. Wolf: Ironmaking Steelmaking, 27 (2000) 450-454

[37] H. Hiebler, C. Bernhard: Steel Research 70 (1999) 349-355

[38] R. Pierer, C. Bernhard, C. Chimani: „Gängige Heissrissbildungskriterien und experimentelle Überprüfung", BHM 149 (2004) 95-101

[39] R. Pierer, C. Bernhard, C. Chimani: "A contribution to hot tearing in the continuous casting process", La Revue de Métallurgie - CIT, February 2007, 72-83

[40] C. Bernhard, G. Xia: "Influence of alloying elements on the thermal contraction of peritectic steels during initial solidification", Ironmaking and Steelmaking 33 (2006) 52-56